Available online at www.sciencedirect.com
ScienceDirect
Polymer 47 (2006) 6606–6621
polymer
www.elsevier.com/locate/polymer

Synthesis, characterization and liquid-crystal-aligning properties of novel aromatic polypyromellitimides bearing (*n*-alkyloxy)biphenyloxy side chains

Seung Beum Lee [a], Gyo Jic Shin [a], Jun Ho Chi [a], Wang-Cheol Zin [a], Jin Chul Jung [a,*], Suk Gyu Hahm [b], Moonhor Ree [b,*], Taihyun Chang [b]

[a] *Polymer Research Institute, Department of Materials Science and Engineering, Pohang University of Science and Technology (POSTECH), San 31, Hyoja-dong, Pohang 790-784, Republic of Korea*

[b] *Department of Chemistry, Pohang University of Science and Technology (POSTECH), San 31, Hyoja-dong, Pohang 790-784, Republic of Korea*

Received 12 April 2006; received in revised form 6 July 2006; accepted 11 July 2006
Available online 9 August 2006

Abstract

Novel aromatic polypyromellitimides bearing (*n*-alkyloxy)biphenyloxy side chains were prepared by two-step polycondensation of 1,4-phenylenediamine (PDA) and biphenyl-4,4′-diamine (BZ) with 3,6-bis[4′-(*n*-alkyloxy)biphenyl-4-oxy]pyromellitic dianhydrides (C_mB-PMDAs, $m = 6$, 8, 10, 12), which had been synthesized by the nucleophilic substitution of *N*,*N*′-diphenyl-3,6-dibromopyromellitimides with sodium 4-(*n*-alkyloxy)biphenoxides. Inherent viscosities of the poly(amic acid)s were in the 0.26–0.62 dL/g range. Poly{1,4-phenylene-3,6-bis[4′-(*n*-alkyloxy)biphenyl-4-oxy]pyromellitimide}s (C_mB-PPIs) and poly{4,4′-biphenyl-3,6-bis[4′-(*n*-alkyloxy)biphenyl-4-oxy]pyromellitimide}s (C_mB-BPIs) obtained in films by thermal imidization of the corresponding poly(amic acid)s were characterized by FT-IR spectroscopy and elemental analysis, and their crystalline structure and thermal properties were measured and discussed with respect to the side chain length. After the polyimide films were surface-treated by rubbing with velvet fibers, standard liquid crystal (LC) cells containing 4-cyano-4′-*n*-pentylbiphenyl (5CB) were fabricated and their LC-aligning properties were investigated in terms of pretilt angle. The pretilt angles were remarkably affected by side chain length and on surface of the polyimides with $m = 6$ and 8 LCs aligned parallel to the rubbing direction while on surface of the polyimides with $m = 10$ and 12 they aligned nearly or completely vertical to the rubbing direction.

Keywords: Polyimides; Polypyromellitimides; Aromatic polyimides

1. Introduction

Aromatic polyimides are widely applied in many fields of advanced technology [1] due to their excellence in mechanical performance and thermal stability as well as liquid crystal (LC) alignability, and gas permeability [2,3]. In recent years, the application as LC-aligning films draws the highest attraction to manufacture the monitors of thin film transistor-liquid crystal display (TFT-LCD) devices for many electronic appliances such as notebook computers or mobile telephones, and the global TFT-LCD devices market is reported to have already exceeded that of Si-based semiconductors [4].

In TFT-LCDs for notebook computers, 90°-twisted nematic modes are the most widely taken in industry. In attaining good quality of the TFT-LCD devices many factors should be taken into account such as viewing angle, optical contrast, response time, and LC alignment stability. However, the high pretilt angle of LC molecules on surface-treated polyimide films is one of the most critical parameters in determining the electro-optical characteristics of TFT-LCD assemblies. The commercial devices are known to require the angles greater than 5° [5,6] and hence many researches have been devoted to develop the new polyimides that can provide high pretilt angles [7–9].

In recent years, the introduction of flexible side chains onto the rigid polymer backbone has attracted a lot of attention

* Corresponding authors. Tel.: +82 54 279 2148; fax: +82 54 279 2399.
E-mail address: jcjung@postech.ac.kr (J.C. Jung).

0032-3861/$ - see front matter © 2006 Elsevier Ltd. All rights reserved.
doi:10.1016/j.polymer.2006.07.036

[7,8,10–12] because a particularly increased interaction between the flexible parts of the polyimides and LC molecules is observed to enhance pretilt angles [9,10,13–16]. To affix flexible side chains to rigid aromatic polyimide backbones, the substitution reaction can be undertaken, in principle, on dianhydride units and/or on diamine units. Up to now most of the side chain incorporations were made on diamine units [15,16], since diamine monomers are to modify more easily than dianhydride monomers [9]. Among aromatic dianhydrides, pyromellitic dianhydride (PMDA) is known to give the highest performance in many properties when incorporated into polyimides [1], but not many works have been reported on PMDA modification. PMDA ring has only two hydrogen atoms available for substitution and each is surrounded by two neighboring carbonyl groups, and hence the reactions for their substitution for attaching side chains are generally difficult [9].

In our laboratory, we have been pursuing the synthesis and polymerization of new PMDAs that are 3,6-disubstituted with various flexible side chains [7–9] and found that the polypyromellitimides result in not only excellent thermal properties but also distinctively higher pretilt angles than those without the side chains [14,17–19]. In this study, we want to report another PMDA modification. For this we synthesized new 3,6-bis[4′-(*n*-alkyloxy)biphenyl-4-oxy]pyromellitic dianhydrides (C_mB-PMDAs, $m = 6$, 8, 10, 12) and polymerized with conventional *p*-phenylenediamine (PDA) and biphenyl-4,4′-diamine (BZ) to obtain poly{1,4-phenylene-3,6-bis[4′-(*n*-alkyloxy)biphenyl-4-oxy]pyromellitimide}s (C_mB-PPIs) and poly{4,4′-biphenyl-3,6-bis[4′-(*n*-alkyloxy)biphenyl-4-oxy]-pyromellitimide}s (C_mB-BPIs), respectively. Synthesis of C_mB-PMDAs with *m* lower than 5 was excluded since these polyimides are too rigid to process and exert little effect on the enhancement of pretilt angles [14,17–19].

To the polypyromellitimides we incorporated not only the flexible alkyl chains but also liquid crystalline biphenyl unit in an attempt to increase the interaction between the biphenyl moieties of the polyimides and the nematic LCs such as 5CB, which is commonly used as a standard LC molecule. The new rigid-rod C_mB-PPIs and C_mB-BPIs were obtained in good-quality films for structural characterization and investigation of properties. From the films, standard LC cells were prepared and their LC-aligning properties were investigated and discussed with respect to their chemical structure.

2. Experimental

2.1. Materials

N-Methyl-2-pyrrolidone (NMP) was distilled at a reduced pressure after stirring over calcium hydride for 24 h. PDA was purified by recrystallization from a mixture of ethanol and water and BZ was used right after sublimation. Methanol was made anhydrous by refluxing over sodium and subsequent distillation. Potassium permanganate, bromine, sodium and aniline were used as received. All the other solvents and chemicals were used without further purification unless otherwise stated.

2.2. Measurements

The melting temperatures were determined using Haake–Buechler melting point apparatus. FT-IR spectra were recorded on a Mattson Infinity Gold spectrophotometer. ^{1}H NMR and ^{13}C NMR spectra were obtained from a 300 MHz Bruker AM 300 spectrophotometer. Elemental analyses were performed on a Elementar Vario EL microanalyzer at the Korea Basic Science Institute (Daegu, Korea). Inherent viscosities were measured with an Ubbelohde-type viscometer at 25 °C in NMP for poly(amic acid)s. Thermal analyses of polyimides were carried out with a Perkin–Elmer PE PC series TGA 7 thermogravimetric analyzer and a PE PC series DSC 7 thermal analyzer at a scanning rate of 10 °C/min under a nitrogen flow. X-ray diffractograms were obtained in a transmission mode using Ni-filtered Cu Kα-radiation on a Rigaku Geiger Flex D-Max X-ray diffractometer.

2.3. Preparation of LC cell and measurement of LC alignment

Polyimide films for LC alignment layers were prepared by spin casting 4 wt.% poly(amic acid) solutions in NMP at 3000 rpm for 40 s onto cleaned ITO glass plates (1.5×4 cm^2), followed by drying, thermally imidizing and detaching by soaking in distilled water. The films were subsequently rubbed with a roller (Wande Co.) covered with a rayon velvet fabric (YA-20-R, Yoshikawa Co., fabric density 2400 fiber/cm^2, fiber diameter 15 μm, and length 1.85 mm) and the rubbing density was calculated by the equation $L/l = N[(2\pi rn/60v) - 1]$, where L (mm) is the total length of the rubbing cloth that touches a certain point of the film, l (mm) is the contact length of the rubbing roller circumference, N is the cumulative number of rubbings, v (cm/s) is the velocity of the substrate stage, and n (rpm) and r (cm) are the rubbing roller speed and radius, respectively.

LC cells were fabricated from two pieces of the rubbed polyimide films (1.5×4.0 cm^2) assembled in an antiparallel rubbing direction at 50 μm cell gap using poly(ethylene terephthalate) film spacers and filled with 5CB containing 1.0 wt.% dichroic dye (Disperse Blue 1) by a capillary method. Optical phase retardation measurements, as described earlier [17], were carried out with a phase retardation analyzer equipped with a photoelastic modulator (model PEM 90, Hinds Instruments) with a fused silica head, a He–Ne laser with a 632.8 nm wavelength (model 106-1, Spectra Physics), a pair of polarizers (model 27300, Oriel), a photodiode detector (model PIN-10DL, UDT Sensors), and a pair of lock-in amplifiers (model SR510, Stanford Research Systems). The pretilt angles for the fabricated LC cells were measured by a crystal rotation method using a laboratory apparatus equipped with a goniometer, a photodiode detector, a He–Ne laser (632.8 nm), a polarizer–analyzer pair, and a sample stage.

2.4. Monomer synthesis

2.4.1. Synthesis of N,N′-diphenyl-3,6-dibromopyromellitimide (*1*)

This raw material was prepared starting from 1,2,4,5-tetramethylbenzene by bromination, oxidation with potassium permanganate and imidization with aniline according to our previous work [7] in 78.6% yield. M.p. > 300 °C.

2.4.2. Synthesis of N,N′-diphenyl-3,6-bis[4-(n-alkyloxy)-biphenyl-4′-oxy]pyromellitimides (*2*)

In a thoroughly dried 500 mL round-bottomed flask equipped with a drying tube, a distillation kit and a gas inlet tube, 0.29 g (12.6 mmol) of sodium were dissolved in 20 mL of anhydrous methanol in N_2 atmosphere and then 12.6 mmol of 4-(*n*-alkyloxy)-4′-hydroxybiphenyls were added and stirred magnetically for 30 min at room temperature. After methanol and water formed were completely distilled out, 250 mL of anhydrous NMP were added. To this solution 5.73 mmol of **1** dissolved in 20 mL NMP were dropped and the mixture was stirred for 24 h. Then the reaction mixture was poured into excess of cold water for precipitation. The precipitates were filtered, washed with water and dried *in vacuo*. They were purified by recrystallization from 1/1 chloroform/methanol mixture.

2.4.2.1. N,N′-Diphenyl-3,6-bis[4-(n-hexyloxy)biphenyl-4′-oxy]pyromellitimide (*2a*)

Yield: 56.2%. M.p. > 300 °C. IR (KBr pellet, cm^{-1}): 2930–2850 (CH, aliphatic), 1772 and 1731 (imide), 1609 and 1497 (aromatic), 1249 and 1208 (C–O–C). ^{1}H NMR (DMSO-d_6, ppm): 0.85–0.90 (t, 6H, $-CH_3$), 1.25–1.49 (br m, 12H, $-(CH_2)_3-CH_3$), 1.63–1.80 (quint, 4H, $-O-CH_2-CH_2-$), 3.94–4.03 (t, 4H, $-O-CH_2-$), 6.97, 7.00, 7.19, 7.22 (dd, 8H, aromatic), 7.36–7.61 (m, 18H, aromatic).

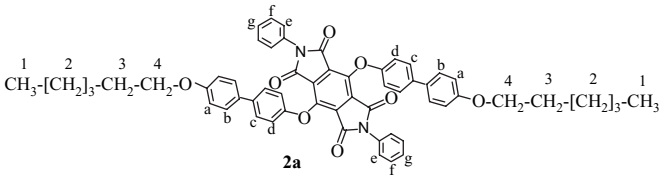

2a

2.4.2.2. N,N′-Diphenyl-3,6-bis[4-(n-octyloxy)biphenyl-4′-oxy]pyromellitimide (*2b*)

Yield: 77.3%. M.p. > 300 °C. IR (KBr pellet, cm^{-1}): 2930–2850 (CH, aliphatic), 1777 and 1731 (imide), 1600 and 1496 (aromatic), 1247 and 1207 (C–O–C). ^{1}H NMR (DMSO-d_6, ppm): 0.82–0.90 (t, 6H, $-CH_3$), 1.25–1.45 (br m, 20H, $-(CH_2)_5-CH_3$), 1.63–1.80 (quint, 4H, $-O-CH_2-CH_2-$), 3.94–4.03 (t, 4H, $-O-CH_2-$), 6.97, 7.00, 7.19, 7.22 (dd, 8H, aromatic), 7.36–7.61 (m, 18H, aromatic).

2.4.2.3. N,N′-Diphenyl-3,6-bis[4-(n-decyloxy)biphenyl-4′-oxy]pyromellitimide (*2c*)

Yield: 61%. M.p. 286–289 °C. IR (KBr pellet, cm^{-1}): 2930–2850 (CH, aliphatic), 1776 and 1731 (imide), 1609 and 1497 (aromatic), 1247 and 1209 (C–O–C). ^{1}H NMR (DMSO-d_6, ppm): 0.80–0.90 (t, 6H, $-CH_3$), 1.15–1.51 (br m, 28H, $-(CH_2)_7-CH_3$), 1.63–1.82 (quint, 4H, $-O-CH_2-CH_2-$), 3.94–4.03 (t, 4H, $-O-CH_2-$), 6.97, 7.00, 7.19, 7.22 (dd, 8H, aromatic), 7.36–7.61 (m, 18H, aromatic).

2.4.2.4. N,N′-Diphenyl-3,6-bis[4-(n-dodecyloxy)biphenyl-4′-oxy]pyromellitimide (*2d*)

Yield: 56.5%. M.p. 273–276 °C. IR (KBr pellet, cm^{-1}): 2930–2850 (CH, aliphatic), 1776 and 1731 (imide), 1609 and 1496 (aromatic), 1249 and 1209 (C–O–C). ^{1}H NMR (DMSO-d_6, ppm): 0.81–0.89 (t, 6H, $-CH_3$), 1.20–1.50 (br m, 36H, $-(CH_2)_3-CH_3$), 1.64–1.80 (quint, 4H, $-O-CH_2-CH_2-$), 3.92–4.03 (t, 4H, $-O-CH_2-$), 6.97, 7.00, 7.19, 7.22 (dd, 8H, aromatic), 7.36–7.60 (m, 18H, aromatic).

2.4.3. Synthesis of 3,6-bis[4′-(n-alkyloxy)biphenyl-4-oxy]-pyromellitic acids (*3*)

In 250 mL round-bottomed flasks with condensers and stirrers, 2–3 g of **2a–d** were dissolved in 100 mL 10% KOH solution (ethanol/water 1/2 v/v mixture). The solutions were refluxed for 12 h, cooled to room temperature and acidified with concentrated HCl solution to precipitate. The precipitates were collected and added into the stirred solutions consisting of 38 mL of concentrated HCl and 200 mL of DMSO. These solutions were stirred at 80 °C for 6 days, cooled to room temperature and poured into excess of cold water. The crude products were obtained by repeated extraction with ethyl acetate and precipitation into *n*-hexane and purified by recrystallization from benzene/ethanol mixtures (2/1 v/v).

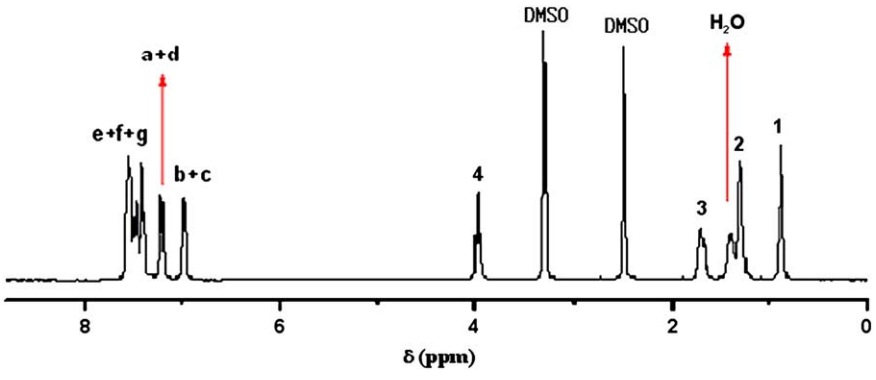

*2.4.3.1. 3,6-Bis[4′-(n-hexyloxy)biphenyl-4-oxy]pyromellitic acid (**3a**)*

Yield: 69.8%. IR (KBr pellet, cm^{-1}): 3600–2300 (br, COOH), 1717 (C=O), 1495 (aromatic), 1244 and 1213 (C–O–C). ^{1}H NMR (DMSO-d_6, ppm): 0.85–0.91 (t, 6H, $-CH_3$), 1.20–1.55 (br m, 12H, $-(CH_2)_3-CH_3$), 1.67–1.82 (quint, 4H, $-O-CH_2-CH_2-$), 3.94–4.04 (t, 4H, $-O-CH_2-$), 6.89, 6.91, 6.98, 7.01 (dd, 8H, aromatic), 7.50–7.62 (m, 8H, aromatic), 13.7 (br, 4H, −COO*H*).

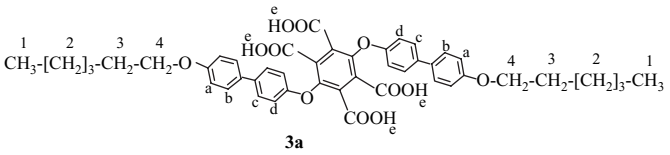

3a

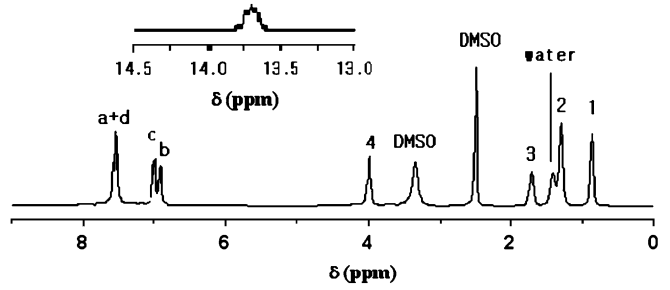

*2.4.3.2. 3,6-Bis[4′-(n-octyloxy)biphenyl-4-oxy]pyromellitic acid (**3b**)*

Yield: 52.4%. IR (KBr pellet, cm^{-1}): 3600–2300 (br, COOH), 1717 (C=O), 1495 (aromatic), 1241 and 1217 (C–O–C). ^{1}H NMR (DMSO-d_6, ppm): 0.83–0.91 (t, 6H, $-CH_3$), 1.20–1.55 (br m, 20H, $-(CH_2)_5-CH_3$), 1.65–1.80 (quint, 4H, $-O-CH_2-CH_2-$), 3.92–4.05 (t, 4H, $-O-CH_2-$), 6.89, 6.91, 6.98, 7.00 (dd, 8H, aromatic), 7.45–7.62 (m, 8H, aromatic), 13.7 (br, 4H, −COO*H*).

*2.4.3.3. 3,6-Bis[4′-(n-decyloxy)biphenyl-4-oxy]pyromellitic acid (**3c**)*

Yield: 40.5%. IR (KBr pellet, cm^{-1}): 3600–2300 (br, COOH), 1718 (C=O), 1495 (aromatic), 1244 and 1215 (C–O–C). ^{1}H NMR (DMSO-d_6, ppm): 0.81–0.93 (t, 6H, $-CH_3$), 1.15–1.55 (br m, 28H, $-(CH_2)_7-CH_3$), 1.65–1.82 (quint, 4H, $-O-CH_2-CH_2-$), 3.94–4.05 (t, 4H, $-O-CH_2-$), 6.89, 6.92, 6.97, 7.00 (dd, 8H, aromatic), 7.47–7.64 (m, 8H, aromatic), 13.7 (br, 4H, −COO*H*).

*2.4.3.4. 3,6-Bis[4′-(n-dodecyloxy)biphenyl-4-oxy]pyromellitic acid (**3d**)*

Yield: 40.0%, IR (KBr pellet, cm^{-1}): 3600–2300 (br, COOH), 1717 (C=O), 1496 (aromatic), 1245 and 1217 (C–O–C). ^{1}H NMR (DMSO-d_6, ppm): 0.80–0.93 (t, 6H, $-CH_3$), 1.15–1.55 (br m, 36H, $-(CH_2)_9-CH_3$), 1.65–1.81 (quint, 4H, $-O-CH_2-CH_2-$), 3.94–4.06 (t, 4H, $-O-CH_2-$), 6.89, 6.91, 6.98, 7.00 (dd, 8H, aromatic), 7.47–7.62 (m, 8H, aromatic), 13.7 (br, 4H, −COO*H*).

*2.4.4. Synthesis of 3,6-bis[4′-(n-alkyloxy)biphenyl-4-oxy]-pyromellitic dianhydrides (**4**)*

In 100 mL round-bottomed flasks with reflux condensers, drying tubes and gas inlet tubes, 0.72–2 g of **3a–d** were dissolved in 40 mL of acetic anhydride. After refluxing for 6 h the reaction mixtures were cooled below room temperature for precipitation. The precipitates were filtered and washed several times with diethylether under stringent exclusion of moisture and dried *in vacuo*.

*2.4.4.1. 3,6-Bis[4′-(n-hexyloxy)biphenyl-4-oxy]pyromellitic dianhydride (C_6B-PMDA) (**4a**)*

Yield: 70%. IR (KBr pellet, cm^{-1}): 2980–2850 (CH, aliphatic), 1857, 1799, 1784 (C=O), 1609 and 1495 (aromatic), 1248 and 1205 (C–O–C). ^{1}H NMR (acetone-d_6, ppm): 0.85–0.94 (t, 6H, $-CH_3$), 1.25–1.56 (br m, 12H, $-(CH_2)_3-CH_3$), 1.71–1.85 (quint, 4H, $-O-CH_2-CH_2-$), 3.98–4.07 (t, 4H, $-O-CH_2-$), 6.96–7.03, 7.19–7.27 (dd, 8H, aromatic), 7.50–7.63 (m, 8H, aromatic).

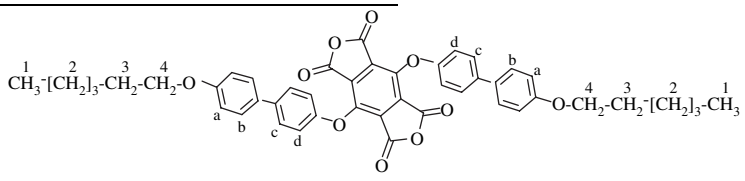

4a C_6B-PMDA

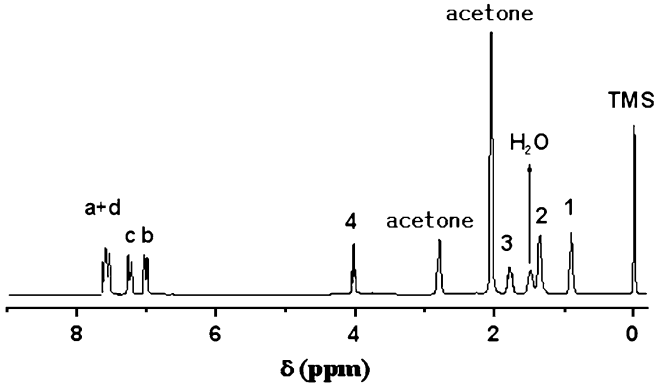

*2.4.4.2. 3,6-Bis[4′-(n-octyloxy)biphenyl-4-oxy]pyromellitic dianhydride (C_8B-PMDA) (**4b**)*

Yield: 75%. IR (KBr pellet, cm^{-1}): 2980–2848 (CH, aliphatic), 1853, 1790, 1780 (C=O), 1600 and 1495 (aromatic), 1245 and 1206 (C–O–C). ^{1}H NMR (acetone-d_6, ppm): 0.85–0.92 (t, 6H, $-CH_3$), 1.25–1.56 (br m, 20H, $-(CH_2)_5-CH_3$), 1.73–1.87 (quint, 4H, $-O-CH_2-CH_2-$), 3.98–4.08 (t, 4H, $-O-CH_2-$), 6.96–7.04, 7.19–7.27 (dd, 8H, aromatic), 7.50–7.65 (m, 8H, aromatic).

*2.4.4.3. 3,6-Bis[4′-(n-dodecyloxy)biphenyl-4-oxy]pyromellitic dianhydride (C_{10}B-PMDA) (**4c**)*

Yield: 76%. IR (KBr pellet, cm^{-1}): 2980–2850 (CH, aliphatic), 1858, 1790, 1785 (C=O), 1609 and 1494 (aromatic), 1248 and 1209 (C–O–C). ^{1}H NMR (acetone-d_6, ppm): 0.82–0.92 (t, 6H, $-CH_3$), 1.22–1.58 (br m, 28H, $-(CH_2)_7-CH_3$), 1.72–1.85 (quint, 4H, $-O-CH_2-CH_2-$), 3.98–4.07 (t, 4H, $-O-CH_2-$), 6.95–7.04, 7.18–7.27 (dd, 8H, aromatic), 7.50–7.64 (m, 8H, aromatic).

*2.4.4.4. 3,6-Bis[4′-(n-dodecyloxy)biphenyl-4-oxy]pyromellitic dianhydride (C_{12}B-PMDA) (**4d**)*

Yield: 69%. IR (KBr pellet, cm^{-1}): 2980–2848 (CH, aliphatic), 1858, 1799, 1784 (C=O), 1606 and 1492 (aromatic), 1249 and 1209 (C–O–C). ^{1}H NMR (acetone-d_6, ppm): 0.82–0.92 (t, 6H, $-CH_3$), 1.20–1.57 (br m, 36H, $-(CH_2)_9-CH_3$), 1.72–1.83 (quint, 4H, $-O-CH_2-CH_2-$), 3.98–4.07 (t, 4H, $-O-CH_2-$), 6.96–7.04, 7.19–7.26 (dd, 8H, aromatic), 7.52–7.63 (m, 8H, aromatic).

2.5. Polymerization

The polymerizations were conducted by the routine two-step procedure. To obtain the precursor poly(amic acid)s 0.5 mmol of the dianhydride monomers were added to stirred solutions of 0.5 mmol of PDA or BZ in anhydrous NMP (solid content 8–15% w/w) under N_2 at room temperature for 24–48 h. The polyimide films were obtained by casting the poly(amic acid)s solutions in NMP onto glass plates, which had been thoroughly cleaned with Alconox solution and then with acetone, and by subsequent drying of NMP at 80 °C for 90 min and heating under N_2 atmosphere at 130 °C for 60 min and 180 °C for 60 min and 250 °C for 60 min.

2.5.1. Poly{1,4-phenylene-3,6-bis[4′-(n-hexyloxy)biphenyl-4-oxy]pyromellitimide} (C_6B-PPI)

IR (film, cm^{-1}) (Fig. 1(a)): 2932 and 2858 (CH aliphatic), 1776 and 1735 (imide I), 1608 and 1496 (aromatic), 1354 (imide II), 1248 and 1203 (C–O–C). Elemental analysis: calcd for $C_{52}H_{46}N_2O_8$ in wt.%: C 75.53, H 5.61, N 3.39 and found: C 75.3, H 6.0, N 3.5.

2.5.2. Poly{1,4-phenylene-3,6-bis[4′-(n-octyloxy)biphenyl-4-oxy]pyromellitimide} (C_8B-PPI)

IR (film, cm^{-1}): 2927 and 2854 (CH aliphatic), 1777 and 1735 (imide I), 1609 and 1495 (aromatic), 1353 (imide II), 1249 and 1204 (C–O–C). Elemental analysis: calcd for $C_{56}H_{54}N_2O_8$ in wt.%: C 76.17, H 6.16, N 3.17 and found: C 75.9, H 5.1, N 3.1.

2.5.3. Poly{1,4-phenylene-3,6-bis[4′-(n-decyloxy)biphenyl-4-oxy]pyromellitimide} (C_{10}B-PPI)

IR (film, cm^{-1}): 2917 and 2852 (CH aliphatic), 1776 and 1729 (imide I), 1608 and 1494 (aromatic),1361 (imide II), 1247 and 1203 (C–O–C). Elemental analysis: calcd for $C_{60}H_{62}N_2O_8$ in wt.%: C 76.73, H 6.65, N 2.98 and found: C 76.4, H 6.4, N 3.0.

2.5.4. Poly{1,4-phenylene-3,6-bis[4′-(n-dodecyloxy)biphenyl-4-oxy]pyromellitimide} (C_{12}B-PPI)

IR (film, cm^{-1}): 2922 and 2852 (CH aliphatic), 1775 and 1736 (imide I), 1608 and 1495 (aromatic), 1354 (imide II), 1246 and 1204 (C–O–C). Elemental analysis: calcd for $C_{64}H_{70}N_2O_8$ in wt.%: C 77.24, H 7.09, N 2.81 and found: C 77.0, H 7.6, N 2.8.

2.5.5. Poly{4,4′-biphenyl-3,6-bis[4′-(n-hexyloxy)biphenyl-4-oxy]pyromellitimide} (C_6B-BPI)

IR (film, cm^{-1}) (Fig. 1(b)): 2930 and 2857 (CH aliphatic), 1775 and 1730 (imide I), 1608 and 1496 (aromatic), 1368 (imide II), 1246 and 1203 (C–O–C). Elemental analysis: calcd for $C_{58}H_{50}N_2O_8$ in wt.%: C 77.14, H 5.58, N 3.10 and found: C 76.8, H 5.8, N 3.1.

2.5.6. Poly{4,4′-biphenyl-3,6-bis[4′-(n-octyloxy)biphenyl-4-oxy]pyromellitimide} (C_8B-BPI)

IR (film, cm^{-1}): 2926 and 2854 (CH aliphatic), 1776 and 1730 (imide I), 1608 and 1496 (aromatic), 1368 (imide II), 1246 and 1203 (C–O–C). Elemental analysis: calcd for $C_{62}H_{58}N_2O_8$ in wt.%: C 77.64, H 6.10, N 2.92 and found: C 78.0, H 7.3, N 2.7.

2.5.7. Poly{4,4′-biphenyl-3,6-bis[4′-(n-decyloxy)biphenyl-4-oxy]pyromellitimide} (C_{10}B-BPI)

IR (film, cm^{-1}): 2929 and 2855 (CH aliphatic), 1776 and 1729 (imide I), 1598 and 1501 (aromatic), 1375 (imide II), 1241 and 1189 (C–O–C). Elemental analysis: calcd for $C_{66}H_{66}N_2O_8$ in wt.%: C 78.08, H 6.55, N 2.76 and found: C 78.0, H 7.3, N 2.7.

2.5.8. Poly{4,4′-biphenyl-3,6-bis[4′-(n-dodecyloxy)biphenyl-4-oxy]pyromellitimide} (C_{12}B-BPI)

IR (film, cm^{-1}): 2929 and 2855 (CH aliphatic), 1776 and 1729 (imide I), 1598 and 1501 (aromatic), 1375 (imide II), 1241 and 1189 (C–O–C). Elemental analysis: calcd for $C_{70}H_{74}N_2O_8$ in wt.%: C 78.48, H 6.96, N 2.61 and found: C 78.5, H 7.2, N 2.7.

3. Results and discussion

3.1. Monomer synthesis

Synthesis of monomeric C_mB-PMDAs ($m = 6$, 8, 10, 12) having two (*n*-alkyloxy)biphenyloxy side chains began from the nucleophilic bromine displacement reaction of *N*,*N*′-diphenyl-3,6-dibromopyromellitimide with sodium 4-(*n*-alkyloxy)biphenoxides in NMP, as shown in Scheme 1. Sodium 4-(*n*-alkyloxy)biphenoxides had been prepared by reaction of *n*-alkylbromides with excess 4,4′-dihydroxybiphenyl in the presence of 10% NaOH.

The nucleophilic substitution reaction proceeded smoothly at room temperature. The starting material 3,6-dibromopyromellitic dianhydride had been previously protected to *N*,*N*′-diphenyldiimide using aniline for successful conduction of the

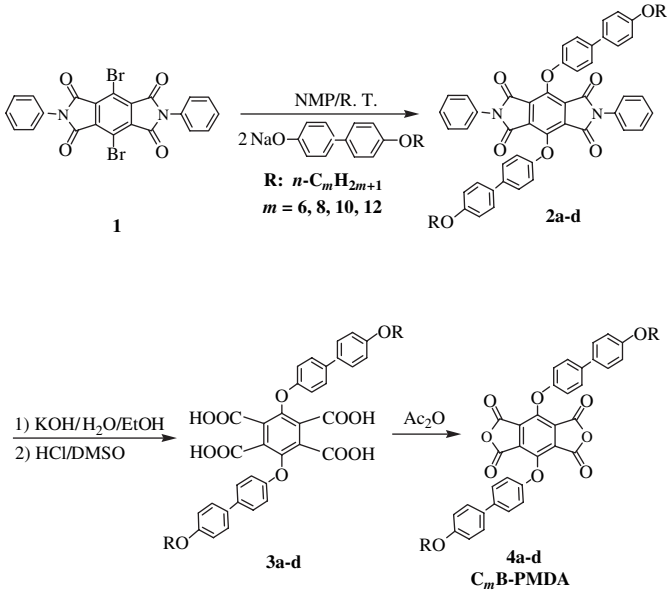

Scheme 1. Synthesis of monomers.

substitution reaction. *N*,*N*′-Diphenyl-3,6-bis[4′-(*n*-alkyloxy)-biphenyl-4-oxy]pyromellitimides produced were deprotected by two-step hydrolysis to the corresponding tetracarboxylic acids. The imide groups were first converted to amic acid groups by base hydrolysis in aqueous 10% KOH solution and then the amic acid groups were further hydrolyzed in concentrated HCl. Thus obtained tetracarboxylic acids were dehydrocyclized to the dianhydrides by treatment with acetic anhydride at room temperature.

To confirm the correct synthesis of C_mB-PMDAs, chemical structures of all the intermediates and products were characterized by FT-IR and ^{1}H NMR spectroscopy. In Section 2, their spectral data are summarized and the ^{1}H NMR spectra of *N*,*N*′-diphenyl-3,6-bis[4′-(*n*-hexyloxy)biphenyl-4-oxy]pyromellitimide (**2a**, Scheme 1, DMSO-d_6), 3,6-bis[4′-(*n*-hexyloxy)biphenyl-4-oxy]pyromellitic acid (**3a**, Scheme 1, DMSO-d_6) and C_6B-PMDA (**4a**, Scheme 1, acetone-d_6) are reproduced together with assignment of each peak. The peak assignments of C_6 derivatives were well coincident with the chemical structures shown in Scheme 1 and all the other C_mB-PMDAs were similar in ^{1}H NMR spectral shape except the increase in relative intensity of the peak for $(CH_2)_{m-3}$ at 1.25–1.56 ppm with increasing *m*. These results indicate that our synthesis yielded the products that had been expected in Scheme 1.

Synthesis of C_mB-PMDAs with *m* lower than 5 was not attempted since the polyimides derived from these dianhydrides have already been known to exert little interaction with LC molecules and hence little effect on the enhancement of pretilt angles [10,13–16].

3.2. Synthesis and characterization of the new polyimides

The new pyromellitic dianhydride monomers C_mB-PMDAs were polymerized with commercially available 1,4-phenylenediamine (PDA) and biphenyl-4,4′-diamine (BZ). As well known, the aromatic parts of both PDA and BZ are so highly rigid that when they are polymerized with C_mB-PMDAs again with rigid backbone, the polyimides are expected to be very poor in solubility in organic solvents. In spite of this expectation the two rigid-rod aromatic diamine monomers were opted as polycondensation counterparts because such aromatic rigid-rod polyimides with flexible side chains are known to be completely dissolution resistant against LC molecules and to give high pretilt angles [14,17–19].

The polymerizations were carried out in two steps in NMP at room temperature under nitrogen flow for 24–48 h, as shown in Scheme 2. With increasing *m* value, polymerization time was extended. During polymerization, the NMP solutions became gradually viscous. At the end of polymerization, small amounts of the obtained precursor poly(amic acid)s were taken off for determining inherent viscosities and the remaining portions were directly cast into thin films onto cleaned glass plates and fully imidized by conventional multi-step thermal treatment method. The films detached from the glass plates by soaking into distilled water after the end of imidization reaction were so tough that they could be highly appropriate for preparing LC cells and measuring their LC-aligning performances.

The polyimide film samples thus obtained were used for characterization by FT-IR spectroscopy and elemental analysis. In Fig. 1 are reproduced the FT-IR spectra of C_6B-PPI and C_6B-BPI films. Both spectra clearly show the characteristic imide I and II bands in the vicinity of 1776, 1735 and 1354 cm^{-1} and C–H stretching vibrations of aliphatic groups in 2930–2850 cm^{-1}. The elemental analysis data determined for C, H and N of the film samples are given in the experimental part. It is to see that the data measured are well coincident with the theoretical ones. These characterization results

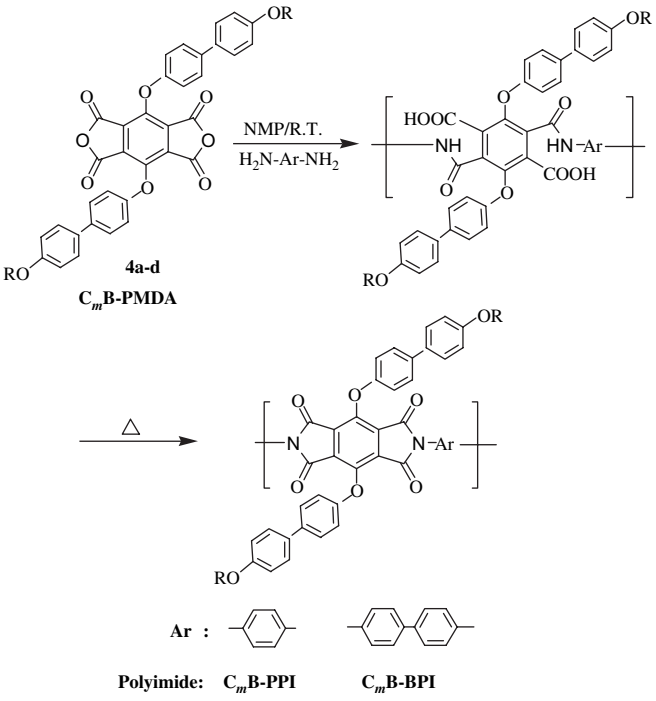

Scheme 2. Polymerization of C_mB-PMDAs.

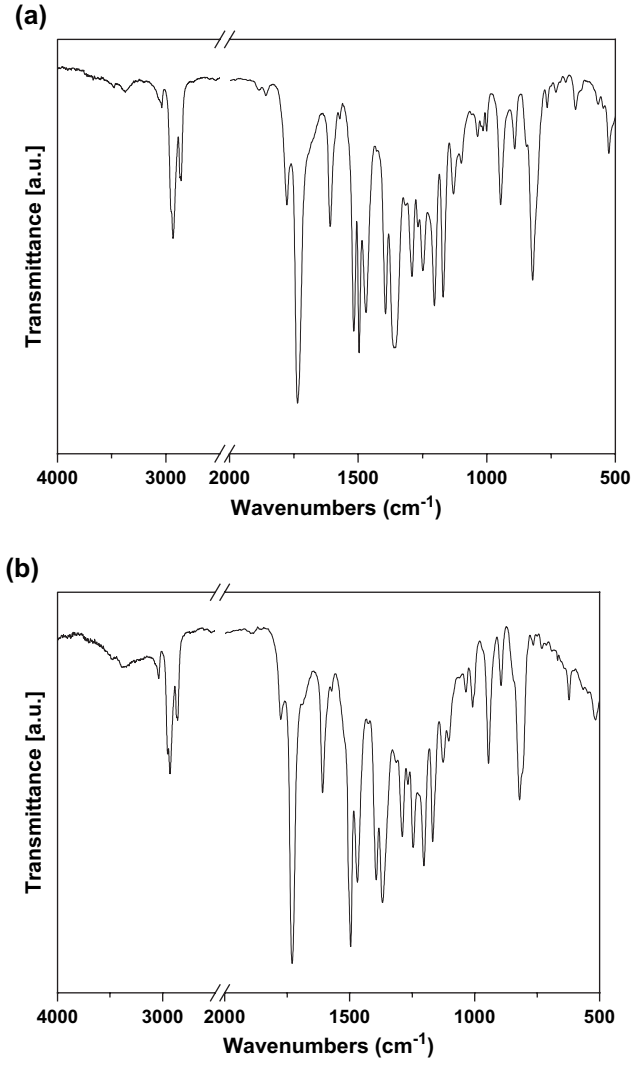

Fig. 1. IR spectrum of (a) C_6B-PPI (film) and (b) C_6B-BPI (film).

indicate that chemical structures of the polyimides prepared coincide well with those given in Scheme 2.

3.3. Structure and properties of polyimides

3.3.1. Solution properties

To make a rough estimation on molecular weights of the polyimides, the inherent viscosities (η_{inh}) of the poly(amic acid)s were determined in NMP at 25 °C and summarized in Table 1. As seen in Table 1, the η_{inh} values of all the poly(amic acid)s with m up to 10 are in the 0.42–0.62 dL/g range, indicating that they must be quite high in molecular weight. However, in spite of extended polymerization time both poly(amic acid)s of C_{12}B-PPI and C_{12}B-BPI gave particularly low η_{inh} value (0.26 dL/g). This behavior might be attributable to the particularly high steric hindrance of *n*-dodecyloxybiphenyloxy group, which hinders diamine nucleophiles from facile approach to C=O group of C_{12}B-PMDA for further propagation. Such sudden drop in η_{inh} has been observed also in the synthesis of rigid-rod poly{*p*-phenylene-3,6-bis[4-(*n*-alkyloxy)-phenyloxy]pyromellitimide}s [7] and poly[tolidine-1,4-diyl-3,6-bis(*n*-alkyloxy)pyromellitimide]s [9] both having *n*-alkyl side groups equal to or higher than dodecyl groups.

Table 1
Inherent viscosity of poly(amic acid)s and thermal behavior of polyimide films

Polymer code	η_{inh} (dL/g)	T_o (°C)	T_{max1} (°C)	T_{max2} (°C)	W_f (%)	W_n (%)	W_s (%)	WR_{800} (%)
C_6B-PPI	0.42	386	458	580	61	76	35	45
C_8B-PPI	0.43	389	452	574	59	71	33	45
C_{10}B-PPI	0.42	386	454	572	51	67	31	37
C_{12}B-PPI	0.26	382	454	579	49	63	29	36
C_6B-BPI	0.46	389	454	581	63	78	40	49
C_8B-BPI	0.55	381	446	588	64	73	38	48
C_{10}B-BPI	0.62	385	446	591	59	69	36	48
C_{12}B-BPI	0.26	356	444	600	57	65	34	47

η_{inh}: Determined at 25 °C in NMP using PAA (0.2 g/dL); T_o: Onset temperature of degradation; T_{max1}: First maximum degradation temperature; T_{max2}: Second maximum degradation temperature; W_f: Residual weight percent found after first degradation; W_n: Calculated residual weight percent to remain after degradation of *n*-alkyloxy group; W_s: Calculated residual weight percent to remain after degradation of (*n*-alkyloxy)biphenyloxy group; WR_{800}: Weight percent remained at 800 °C.

For polyimides to be appropriate as LC-aligning films, they must be completely insoluble and unswellable in LC molecules and their solubilities in various organic solvents were qualitatively determined. All the polyimides were not soluble in common organic solvents such as NMP, DMSO or DMAc even on heating. Even in concentrated sulfuric acid they were only slightly soluble at elevated temperatures. Such poor solubility might be ascribed for very high rigidity of the wholly aromatic poly(*p*-arylenepyromellitimide) backbones, and the attachment of the flexible *n*-alkyloxy side branches brought about only minor effect on enhancement of solubility of the polymers.

To check swellability in LC molecule, all the polyimide films were soaked in 5CB for 72 h at ambient temperatures and their weights were determined before and after soaking and compared with each other, but no detectable changes in weight were noticed even in C_{12}B-PPI and C_{12}B-BPI with the lowest inherent viscosity. This indicates that the polyimides can be safely used for fabricating LC cells.

3.3.2. Thermal behaviors

Thermal stabilities of the polyimide films were studied by TGA and their pyrograms are reproduced in Fig. 2 and their numerical results are summarized in Table 1. As Fig. 2 shows, all the polyimides begin to degrade at temperatures higher than 380 °C, signifying that our new polyimides are excellent in thermal stability.

Fig. 2 shows also that all the samples pyrolyze in two steps, the first step at lower temperatures, presumably to be ascribable for degradation of side chains, and the second step at higher temperatures, probably resulting from pyrolysis of the rigid aromatic backbones. To see in greater detail which parts of side chains degrade in the lower temperature range, we calculated weight percent to remain after degradation of *n*-alkyloxy groups (W_n) and those of (*n*-alkyloxy)biphenyloxy group (W_s) and compared with the remaining weight percent (W_f) observed from the first step degradation. These values are

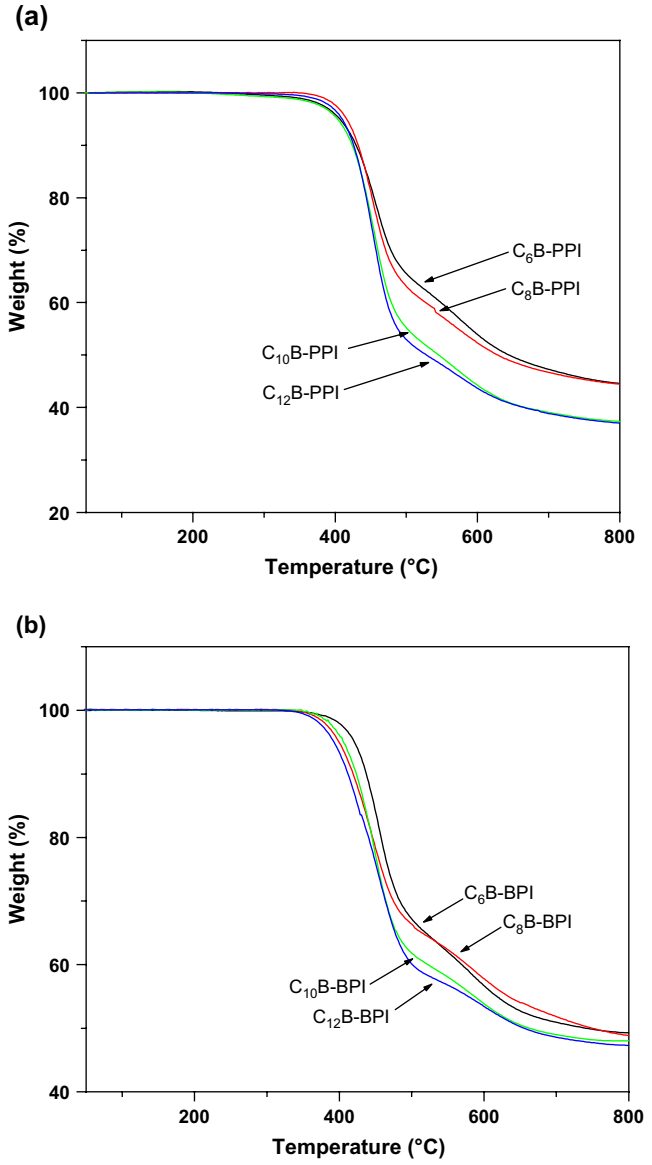

Fig. 2. TGA thermograms of C_mB-PPIs (a) and C_mB-BPIs (b).

summarized also in Table 1. As it shows, the observed W_f values lie between the two W_n and W_s values. This fact means that no single side group selectively degrades away in the low temperature range. To obtain more accurate understanding of the thermal pyrolysis behaviors, more detailed studies are required.

Phase transitions of the polyimides were studied by DSC scanned in nitrogen stream. Their DSC thermograms did not give any detectable phase transitions below degradation temperatures even on repeated scans of the samples after annealed at 200 °C for 24 h. The absence of phase transitions might be ascribable for high rigidity of the wholly aromatic backbones, and they must presumably lie higher than their degradation temperatures.

3.3.3. Crystalline structure

As well known, rigid-rod polymers with flexible side brushes like our C_mB-PPIs and C_mB-BPIs strongly tend to form layered crystalline structure in solid state [7,8,10–12]. If a layer structure is perfectly developed with high degree of crystallinity, the main chains get together to form a rigid backbone domain and the flexible *n*-alkyl side chains fill the space between the rigid backbones in fully extended zigzag configuration to form their own crystalline phase. In the phase, the side chains can be interdigitated with those emanating from neighboring backbones, the degree of interdigitation being governed by chemical structure of the rigid-rod polymers [8,10,12,24]. Therefore a layer structure can be experimentally characterized by measuring the spacings between rigid backbones, which increase with increasing *n*-alkyl side chain length. The increase rate depends on the degree of interdigitation of side chains [10,12,24].

Such layer structures of our polyimides were investigated by wide-angle X-ray diffractometry and the diffractograms obtained from as-polymerized film samples are reproduced in Fig. 3. Fig. 3 shows that all the C_mB-PPIs and C_mB-BPIs have a fairly sharp peak at $q = 5.4\ \text{nm}^{-1}$ corresponding to the Braag spacing (d) of 11.6 Å and at $q = 4.1\ \text{nm}^{-1}$ corresponding to the *d*-spacing of 15.3 Å, respectively. These *d*-spacings are ascribable for the repeat unit length of aromatic backbone [23]. The repeat unit lengths of poly(*p*-phenylenepyromellitimide) (PPI) and poly(4,4′-biphenylpyromellitimide) (BPI) of the same backbone structure as ours but both without side chains are reported to be 12.3 Å and 16.6 Å, respectively [23]. When the repeat unit lengths of our side-chained C_mB-PPIs and C_mB-BPIs are compared with those of bare PPI and BPI, respectively, they are quite well coincident with each other. This coincidence is natural because incorporation of a side chain may cause little change in repeat unit length.

The smallest-angle peak in X-ray diffractogram is the most characteristic of a layered crystalline structure because it arises from the *d*-spacing between rigid backbones. From Fig. 3 it is to see that the smallest-angle peaks from the polyimides with shorter *n*-alkyl side chain lengths are broader than those from the polyimides with longer *n*-alkyl side chain lengths. This indicates that in the former polyimides the interaction of short flexible side chains with rigid backbones is too weak for the layered structures to develop well, while in the latter polyimides the interaction of long flexible side chains is so strong that the layered structures are developed more tightly. Such behavior has been observed also in other rigid-rod polymers with flexible side chains [10–12].

From Fig. 3 it is also to see that in both C_mB-PPIs and C_mB-BPIs the smallest-angle reflections shift to lower angles as the *n*-alkyloxy side chains become longer. This means that the corresponding *d*-spacing between backbones increases with increasing side chain length, and the Braag *d*-spacings were obtained from the smallest-angle peaks of Fig. 3 and plotted against m of *n*-alkyl side chains. This plot is reproduced in Fig. 4. From Fig. 4 it is to confirm that in both C_mB-PPIs and C_mB-BPIs, the *d*-spacing increases linearly with increasing *m*, signifying clearly that layer structures, loose or tight, are formed in our polyimides.

In Fig. 4 it is also to see that for the same *m* values *d*-spacings are generally greater in C_mB-BPIs than in C_mB-PPIs. If

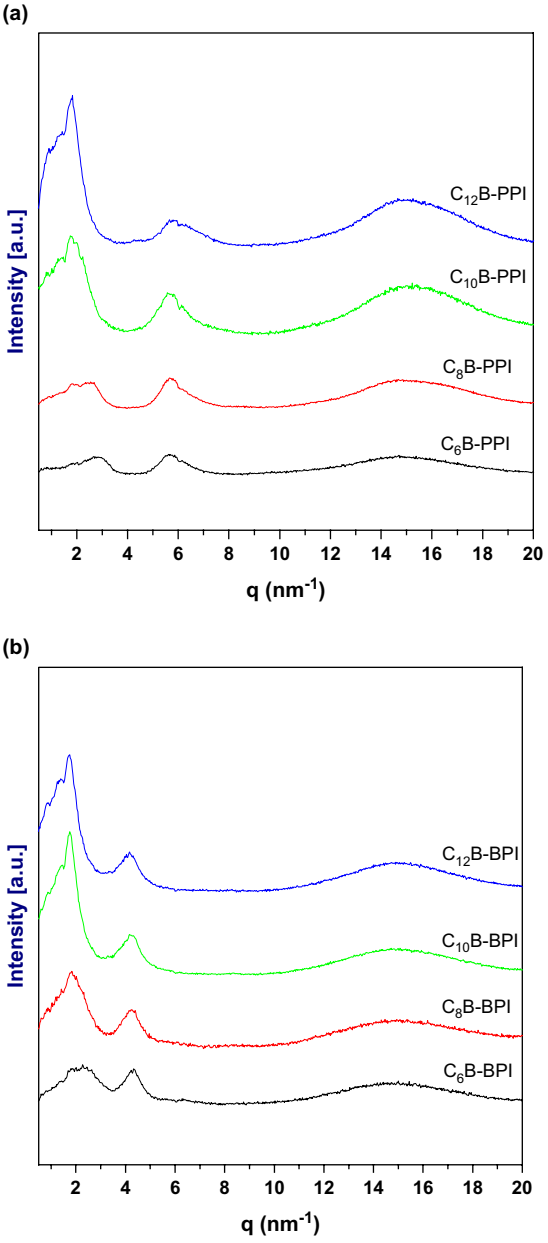

Fig. 3. WAXS diffractograms of C_mB-PPIs (a) and C_mB-BPIs (b).

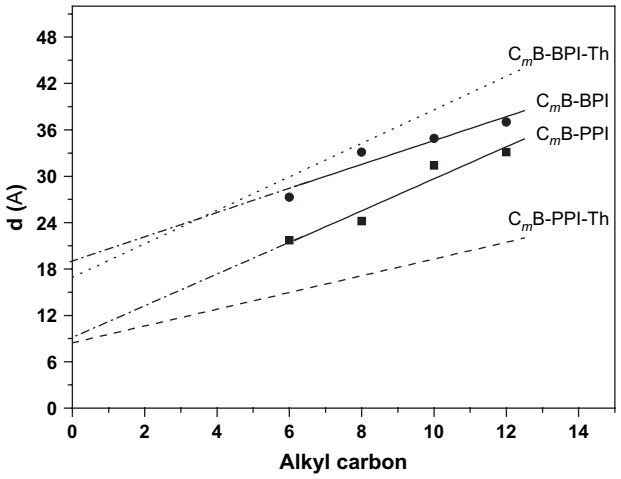

Fig. 4. Plot of d-spacings against m. Calculated: C_mB-BPI-Th and C_mB-PPI-Th and measured: C_mB-BPI and C_mB-PPI.

the n-alkyl side chains are interdigitated to the same degree in both polyimides, the two d values for an m should be identical, because both phenylene unit in C_mB-PPIs and biphenyl unit in C_mB-BPIs are *para*-linked to form linear backbone layer, even though they differ in length. Therefore, it could be conjectured that in C_mB-PPIs the degree of interdigitation of n-alkyl chains must be higher than in C_mB-BPIs.

The linearity of C_mB-PPIs of Fig. 4 has an intercept of 9.1 Å and a slope of 2.07 Å per carbon atom, while that of C_mB-BPIs has 19.2 Å and 1.55 Å per carbon atom, respectively. To analyze the linearities of Fig. 4 we assumed the side chain conformation as drawn in Scheme 3(a), in which length of 4,4′-dioxybiphenyl unit = 9.78 Å, size of a CH_2 unit = 1.25 Å [24], side chain tilt angle = 120° or −60° to the backbone layer or 30° perpendicular to the backbone axis and azimuthal angle = 90°. We assumed further that the 4′-(n-alkyloxy)biphenyl-4-oxy side chains are interdigitated 100% in C_mB-PPIs and 0% in C_mB-BPIs, even though for convenience the assumed layer structure is shown in Scheme 3(b) for C_6B-polyimide with intermediate degree of side chain interdigitation. In Scheme 3(b) a 4′-(n-hexyl)biphenyl-4-oxy side chain bound at C_3 position of pyromellitimide ring is drawn to extend above the backbone plane while the other side chain bound at its C_6 position is oriented below the backbone plane so that in a repeat unit two side chains form more stable transoid conformation than less stable cisoid conformation.

The tilt angle of 120° is reasonable to assume since an ether bond of C_p—O—C_b, where C_p is the carbon atom of pyromellitic ring at 3- or 6-position and C_b is the carbon atom of branched biphenyl ring at 4-position, has an angle close to 120°. Taking into account that a side chain bound to O atom over C_b rotates steadily around C_p—O bond at 120° angle along the periphery of the rotation cone, as depicted in Scheme 3(a), the side chain should be aligned protruded either above or below the backbone plane at a certain azimuthal angle in its stable conformation. If the angle is 0°, the side chain becomes coplanar with backbone plane, but because of the strong steric hindrance from pyromellitic C═O groups this coplanar conformation is improbable. This steric hindrance can be minimized when the side chain is aligned perpendicularly to the backbone layer at an azimuthal angle of 90°, as depicted in Scheme 3(a).

Based on the assumed structure shown in Scheme 3 and degree of side chain interdigitation 0% in C_mB-BPIs and 100% in C_mB-PPIs, the d-spacing of C_{12}-BPI, for instance, was calculated to be $2 \sin 60°[9.78+(12 \times 1.25)] = 42.9$ Å and that of C_{12}-PPI to be $\sin 60°[9.78+(12 \times 1.25)] = 21.5$ Å. For other side chain lengths, the same calculations were conducted and their results are plotted also in Fig. 4 (C_mB-BPI-Th and C_mB-PPI-Th). In Fig. 4 it is to see that compared with the theoretically calculated d values the experimentally measured d values are slightly smaller in C_mB-BPIs while much larger

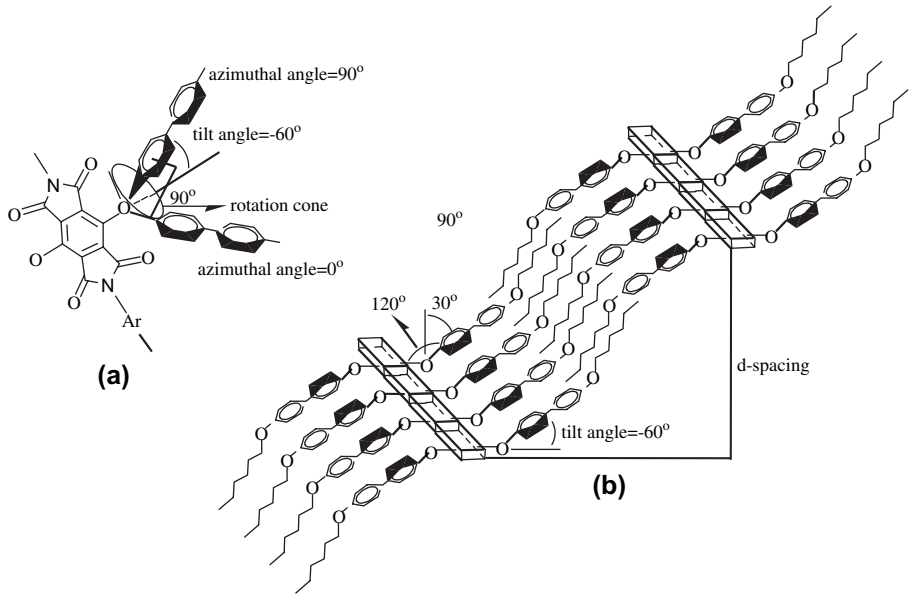

Scheme 3. The side chain alignment (a) and layer structure (b) assumed to calculate theoretical *d*-spacings. For degree of side chain interdigitation see text.

in C_mB-PPIs. This result must signify that the actual degree of side chain interdigitation is slightly higher than 0% in C_mB-BPIs and much lower than 100% in C_mB-PPIs. However, in both the polyimides the difference between measured *d* values and theoretical *d* values decreases with decreasing *m* and the intercepts of 19.2 Å and 9.1 Å determined by extrapolating the measured *d* values of C_mB-BPIs and C_mB-PPIs to $m = 0$ are quite well coincident with 17.2 Å and 8.6 Å calculated theoretically for C_0B-BPI-Th and C_0B-PPI-Th, respectively. These coincidences signify that in C_0B-BPI the side 4,4′-dioxybiphenyl groups must not be interdigitated at all while in C_0B-PPI the side 4,4′-dioxybiphenyl groups must be fully interdigitated with each other.

The big difference in degree of side chain interdigitation between C_mB-BPIs and C_mB-PPIs might be ascribable for the difference in repeat unit length and interchain attraction. The repeat unit length (11.6 Å) of C_mB-PPIs is shorter than that (15.3 Å) of C_mB-BPIs. This means that the side chains are more densely populated in C_mB-PPIs along their main chains than in C_mB-BPIs, indicating that C_mB-PPIs have less free volume in the space between neighboring backbones than C_mB-BPIs. Due to a steric repulsion the less free volume should be less favorable for increasing degree of side chain interdigitation, and this factor leads to the deduction that C_mB-PPIs should have lower degree of the interdigitation than C_mB-BPIs.

Interchain attraction is a qualitative measure of the hydrophobic interaction between two rigid aromatic main chains. In our polyimides, the pyromellitimide ring with three-ring fused structure is distinctively more rigid than *p*-phenylene unit or 4,4′-biphenyl unit, and the main chain rigidity should be higher in C_mB-PPIs than in C_mB-BPIs for an *m*, because in repeat units C_mB-PPIs have one *p*-phenylene unit less than C_mB-BPIs and hence the relative pyromellitimide unit contents are higher in C_mB-PPIs than in C_mB-BPIs. This stronger interchain attraction brings two neighboring main chains closer to each other to enhance the degree of interdigitation of the side chains.

When the negative influence of the less free volume and the positive factor of higher interchain attraction for higher degree of side chain interdigitation in C_mB-PPIs than in C_mB-BPIs are compared against each other, our experimental result seems to be determined more dominantly by the positive factor.

The deduction that side chains of C_m-BPIs are interdigitated more than 0% and side chains of C_m-PPIs are interdigitated far less than 100% can be reconfirmed by the slopes of the linearities. As Fig. 4 shows, in C_m-BPIs the measured slope of 1.55 Å per C atom is smaller than the theoretical slope of 2.16 Å per C atom and in C_m-PPIs the measured slope of 2.07 Å/C is much larger than the theoretical slope of 1.08 Å/C. At this stage, however, calculation of an accurate degree of side chain interdigitation is not feasible in both the polyimides, and further detailed structural studies are required.

As already stated above, the theoretical calculation of *d*-spacings was carried out under the assumption that the *n*-alkyl side chains are fully extended in zigzag configuration and its results have been shown to match quite well with the experimental results. However, as to see from Fig. 3, in wide-angle region at $q = 14-16\ \mathrm{nm}^{-1}$ all the polymers show only broad reflections, indicating that our polyimides are very low in crystallinity and hence the *n*-alkyl side chains do not form their own crystalline domain. Such low crystallinities indicate that the *n*-alkyl side chains are not regularly aligned in side chain domain.

To increase the degree of crystallinity, the films were annealed over prolonged period of time at 200 °C in argon atmosphere, but no distinctive changes were noticed in the wide-angle X-ray diffractograms. This experimental result signifies that the interchain attraction between the very rigid backbones of the polyimides is so strong that even the *n*-alkyl

side chain domains could not be annealed at temperatures lower than their degradation temperatures. Such unannealable behavior has been frequently observed in many other rigid-rod polymers with flexible side chains [7,10,12].

3.4. LC alignment

3.4.1. Surface morphology

Surface morphology of all polyimide films with $5 \times 5\ \mu m^2$ area was measured by AFM before and after rubbing at a density of 120. In Fig. 5(a) and (b) are reproduced the AFM images of C_{10}B-PPI as well as their depth profiles taken along the white lines drawn in the images for unrubbed and rubbed samples, respectively. Fig. 5(a) shows that the unrubbed film surface is highly smooth and uniform, while Fig. 5(b) clearly shows that the rubbed film surface contains many microgrooves, the largest with about 32 nm width at 1.2 μm. All the other polyimides gave the images essentially similar to Fig. 5, although the average sizes of microgrooves appeared slightly different from each other.

The morphology of C_{10}B-PPI surface results from the deformational response of polyimide films to the mechanical shear force induced by the pressed rubbing with the velvet fibers, and thus the degree of deformation should be dependent on ductility of the polyimide material on surface. The fully rod-like PPI and BPI without any flexible side chains is known hard to deform by rubbing [20]. Our C_mB-PPIs and C_mB-BPIs have the same backbone structure as PPI and BPI, respectively, but they are readily deformed by rubbing to generate microgrooves, small or large, on their surfaces. This means that C_mB-PPIs and C_mB-BPIs are more ductile than PPI and BIP on their surfaces. Such ductility should be ascribed for the effect of appendance of the flexible side chains to the rigid backbone.

3.4.2. Birefringence

The fact that microgrooves are formed on polyimide surface by rubbing signifies that some parts of polyimide chains are reoriented by the mechanical deformation along the rubbing direction. This reorientation was examined by the optical birefringence measured in terms of optical phase retardation (birefringence × phase) using He–Ne laser at 632.8 nm. In Fig. 6 are shown polar diagrams taken from the optical phase retardation measured upon in-plane rotating C_mB-PPI and C_mB-BPI films that were rubbed at a density of 60.

A polar diagram like Fig. 6 provides information on the rubbing-induced reorientation of polymer chains on the film surface. As Fig. 6 shows, the signal intensity of all the polyimide films reaches a maximum value at rotating angles of 0° and 180° and a minimum value at 90° and 270°. The same measurements made for unrubbed films revealed no such anisotropic orientation at all. The anisotropy means that the mechanical rubbing induced a noticeable change in reorientation of polyimide chains parallel along the rubbing direction. Such an anisotropic reorientation has also been observed in many other rigid-rod polyimides with flexible side chains [18,19]. This chain reorientation is known to greatly

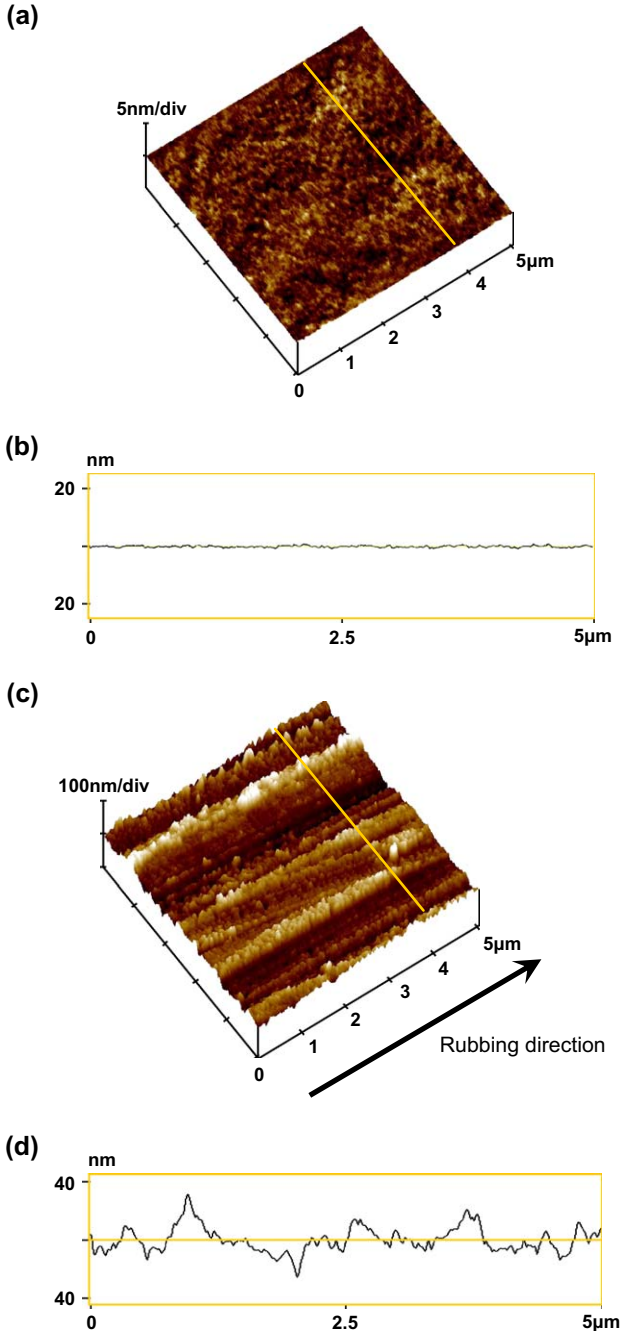

Fig. 5. AFM image of unrubbed C_{10}B-PPI film (a) and its depth profile (b) and AFM image of C_{10}B-PPI film rubbed at a density of 120 (c) and its depth profile (d).

affect LC-aligning ability and direction of the polyimide films [7]. However, which part of the polyimide chains comprising rigid main chain and the side chains having both flexible *n*-alkyl units and rigid biphenyl unit contributes more to the birefringence should be considered thoughtfully.

In birefringence study of poly{*p*-phenylene-3,6-di[4-(*n*-octyloxyphenyl)oxy]pyromellitimide}s (C_mP-PIPs), which have one *p*-phenylene unit less than C_mB-PPIs in their side chains, using polarized FT-IR spectroscopy, it was found that a polar diagram obtained at 1364 cm^{-1} (stretching vibration of C–N bond in main chain) has roughly the same shape as one of

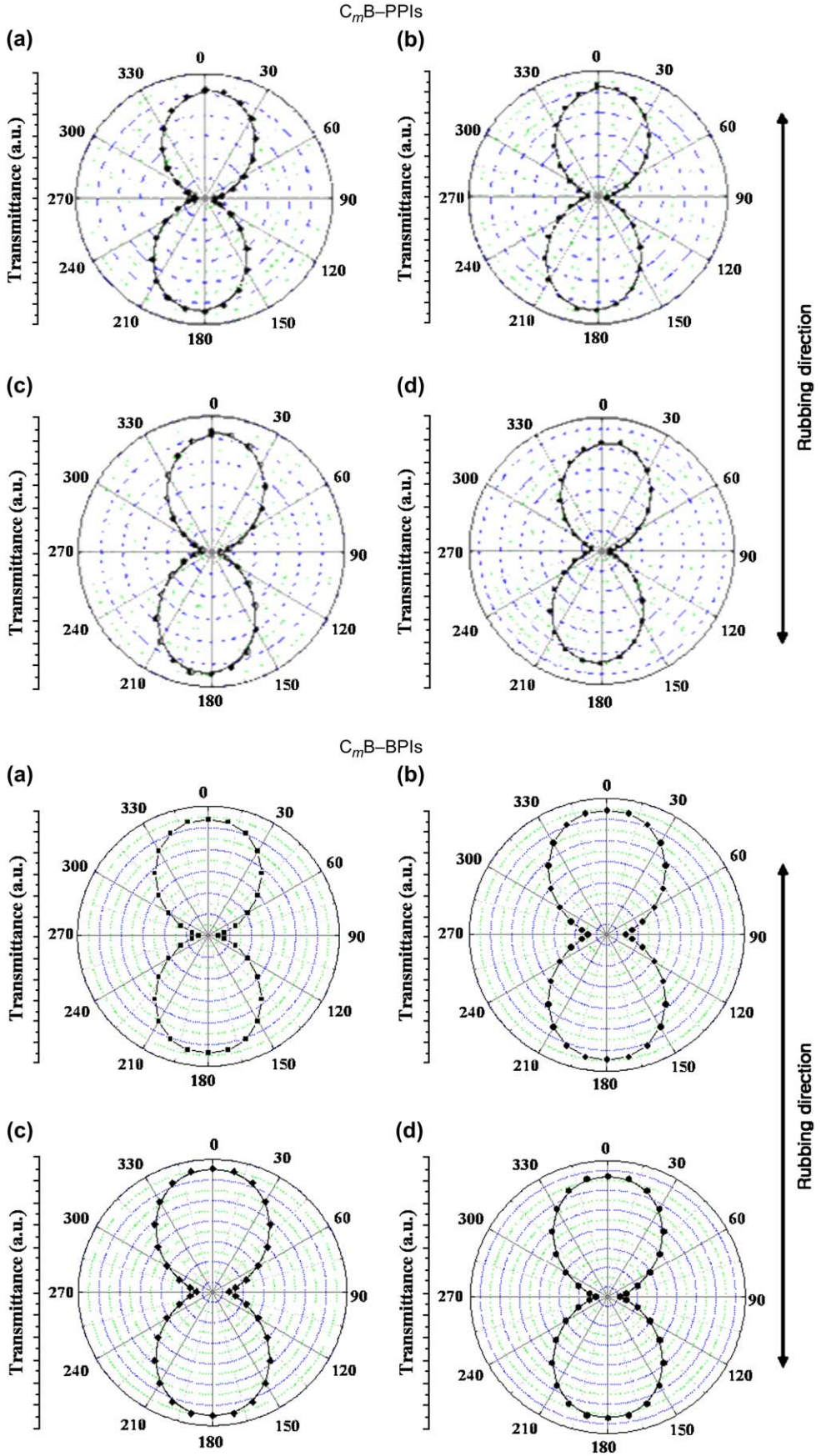

Fig. 6. Polar diagrams taken from the optical phase retardation measurement of polyimide film surfaces rubbed at a density of 60: (a) $m = 6$, (b) $m = 8$, (c) $m = 10$, and (d) $m = 12$.

Fig. 6 while a polar diagram obtained at 2923 cm^{-1} (CH_2 stretching vibration) showed almost completely circular shape [18,19]. This means that the rubbing reorients the rigid main chains along the backbone direction more than the (*n*-octyloxy)phenyloxy side chains [18,19], because the rigid main chains with high glass transition temperature stay as reoriented while the flexible *n*-octyl chains are so mobile that they easily return to stable conformation from reoriented conformation. This report leads us to the similar inference since our polyimides belong to the same category of rigid-rod polymers with flexible side chains.

By rubbing, the tilt angle of 120° of the side chains cannot be distorted in the layered crystal structure (see Scheme 3(a)), but the azimuthal angle can be varied from 90° (perpendicular to backbone layer) maximal to 0° (parallel to and coplanar with the backbone layer). But since an azimuthal angle 0° is not allowable due to the strong steric hindrance from pyromellitic C═O groups, the side chains should be reoriented to the alignment with the azimuthal angle lower than 90° but higher than 0°.

A side chain of our polyimides comprises a rigid *p*-dioxybiphenyl unit and a flexible *n*-alkyl unit. The rigid unit must be less mobile than the flexible unit, and once the side chain is reoriented as the whole by rubbing, the rigid unit must be more probable to remain as reoriented while the flexible unit must be more probable to return back to its stable conformation. In addition, in the polyimides with shorter *n*-alkyl side chains, backbone–backbone distance is shorter, and hence the inter-backbone attraction is so much increased that they are more probable to stay as reoriented, while the reverse is true in the polyimides with longer *n*-alkyl side chains, and they should tend to return back to stable conformation from reoriented conformation more easily. In stable conformation, the azimuthal angle must be 90° to minimize the steric repulsion, and the longer *n*-alkyl side chains should be realigned vertical to the backbone layer even after rubbing. Therefore, if polar diagrams of the polyimides with longer *n*-alkyl side chains are measured using polarized IR light at 2923 nm^{-1}, they should be of nearly circular shape. Such FT-IR studies are under way now.

3.4.3. LC-aligning direction

To investigate the ability of the polyimide films to align LC molecules, 50 μm thick LC cells were fabricated by filling 5CB and 1 wt.% of Disperse Blue 1. The dye is known to align with 5CB molecules always in the same direction. Using the cells, the direction of LC alignment was first determined by polar diagrams taken from the optical phase retardation measurements. In Fig. 7 are reproduced the polar diagrams of the linearly polarized He/Ne laser light absorbance of Disperse Blue 1 as a function of rotational angle of the cell fabricated from the polyimide films.

Fig. 7 shows that in the LC cells made from all the C_6B- and C_8B-polyimide films the absorbance reaches maximum at rotation angles of 0° and 180° and minimum at 90° and 270°, meaning that the LC molecules are aligned parallel along the rubbing direction, whereas in the LC cells made from C_{10}B- and C_{12}B-polyimide films the polar diagrams appear oval with only slight expansion to the rubbing direction, meaning that the LC molecules are aligned almost vertical to the rubbing direction.

In Figs. 5 and 6 it was shown that the mechanical rubbing induced both microgrooves and anisotropic birefringence to align parallel along the rubbing direction. Therefore, it appears easy to interpret that LC alignment parallel to the rubbing direction on rubbed surfaces of the C_6B- and C_8B-polyimides is influenced either/both by anisotropic chain reorientation or/and microscopic grooves, while it is not easy to explain why LC molecules align vertical to the rubbing direction on surface of the C_{10}B- and C_{12}B-polyimides.

In the LC alignment studies with C_8P-PPI [17,18], it was evidenced that the chain reorientation on polyimide film surfaces has greater influence on LC-aligning ability than microgrooves, because the molecular dimension of 5CB (about 1.8 nm long and 0.25 nm thick) is comparable to that of polyimides repeat units and their side chains, but far much smaller than the microgrooves with nanometer sizes. This signifies that to explain the vertical LC alignment in C_{10}B- and C_{12}B-polyimides, their side chain conformations on surface should be considered.

As discussed in birefringence section (3.4.2), the rigid backbones and side *p*-dioxybiphenyl units could remain as reoriented by the rubbing, but the flexible side *n*-alkyl parts with enough length could return back to their stable conformation, in which they are aligned almost vertical to backbone layer. Therefore, the flexible *n*-pentyl unit of 5CB molecules should strongly interact with the vertically aligned *n*-decyl and *n*-dodecyl units on surfaces of the C_{10}B- and C_{12}B-polyimides to result in the vertical LC alignments.

In LC-aligning behavior, C_mP-PPIs with *n*-alkyl length shorter than *n*-octyl showed the parallel alignment to the rubbing direction while those with *n*-decyl and *n*-dodecyl groups gave the completely vertical alignment [17,18], meaning that in the polyimides the critical *n*-alkyl side chain length was *n*-octyl. In our C_mB-PPIs and C_mB-BPIs the critical *n*-alkyl length is one ethylene unit higher than in C_mP-PPIs. This difference cannot be explained accurately at this stage, but it must be related with the fact that our C_mB-PPIs and C_mB-BPIs have one rigid *p*-phenylene unit more than C_mP-PPIs in side chain.

3.4.4. Pretilt angle

Pretilt angles were measured by a crystal rotation method and their numerical values are plotted against rubbing density, as shown in Fig. 8 for C_mB-PPIs (a) and for C_mB-BPIs (b). In Fig. 8 the dark zone arises from the limitation of measurement using our equipment. Fig. 8 shows that the angles of both C_mB-PPIs and C_mB-BPIs with $m = 10$ and 12 are so high that LCs are aligned practically vertical to the rubbing direction, while the angles of both C_mB-PPIs and C_mB-BPIs with $m = 6$ and 8 are so low that LCs are aligned practically parallel to the rubbing direction. This result was to predict from the LC-aligning direction measurements that are described in Section 3.4.3.

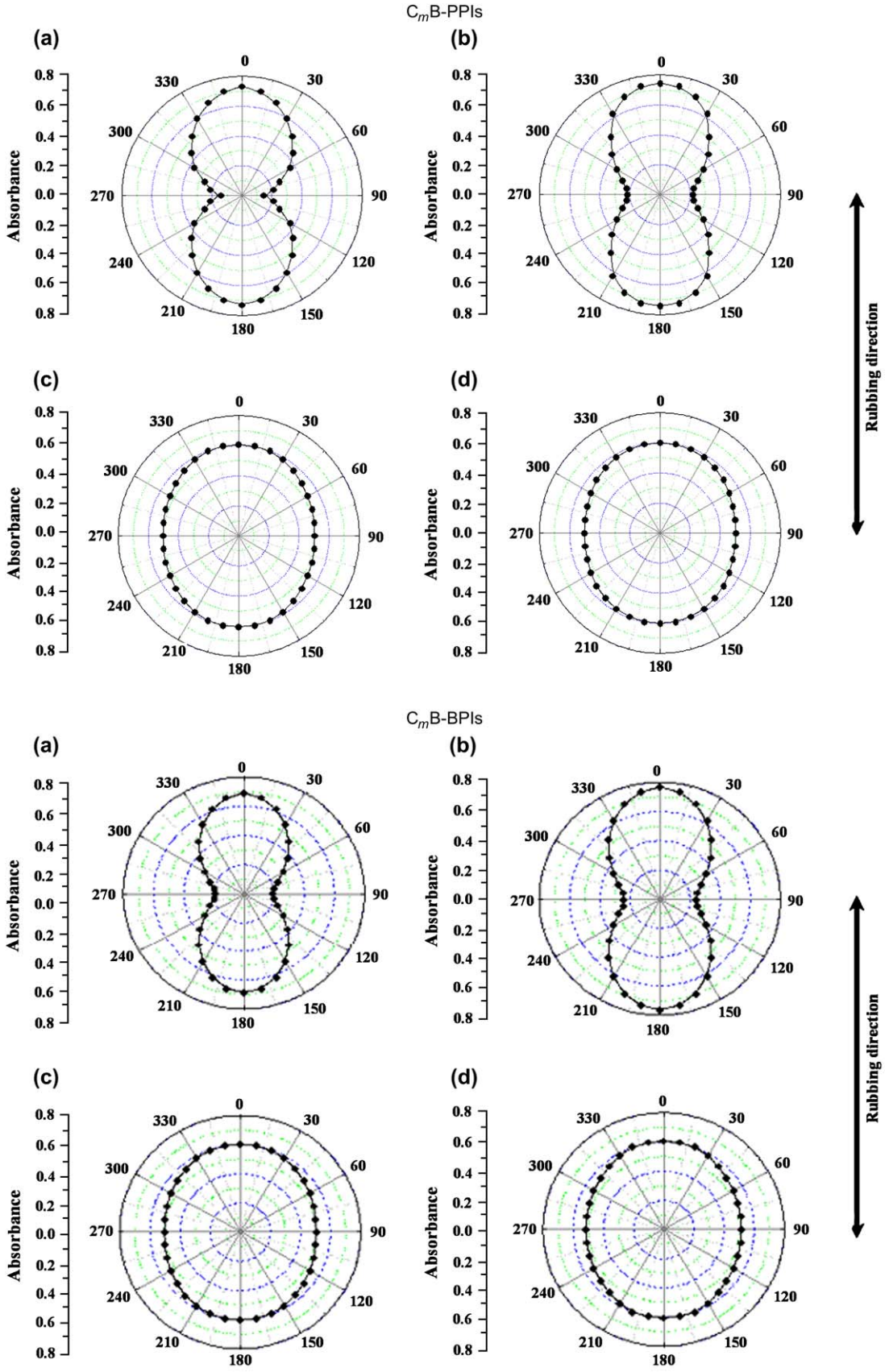

Fig. 7. Polar diagrams for measurement of LC alignment direction for polyimide films rubbed at a density of 60: (a) $m = 6$, (b) $m = 8$, (c) $m = 10$, and (d) $m = 12$.

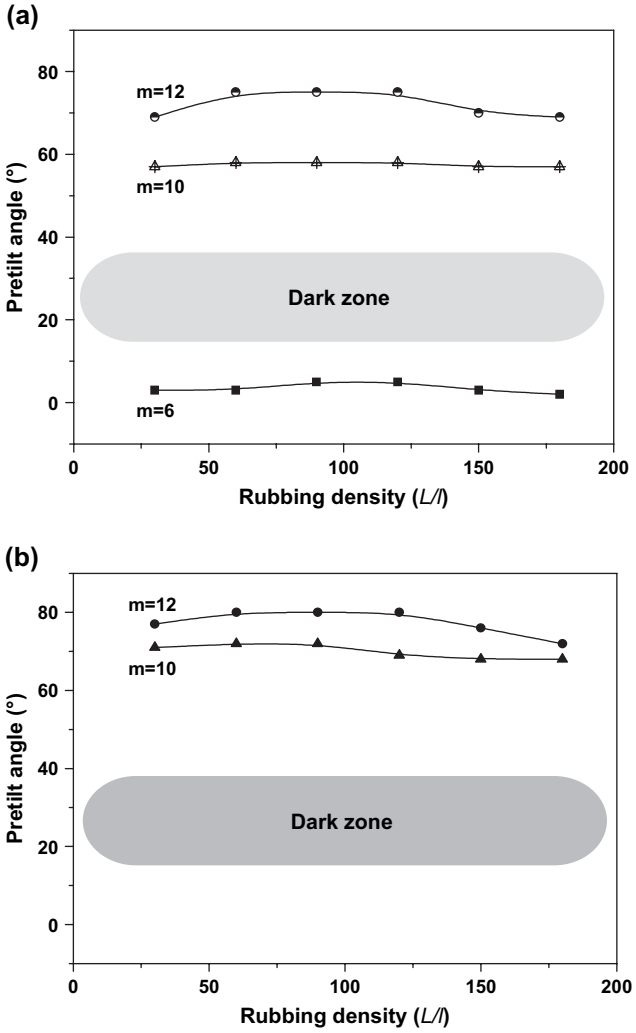

Fig. 8. Pretilt angles of LC on rubbed surfaces of C_mB-PPIs (a) and C_mB-BPIs (b).

Fig. 8 shows also that the angle of each C_mB-BPIs lies slightly higher than that of each C_mB-PPIs, meaning that the interaction of the side chains of C_mB-BPIs with 5CB molecules is slightly higher than that of C_mB-PPIs. It was reported [17,18,20–22] that a pretilt angle of LC molecules is affected mainly by van der Waals interactions and the inclination angle of polymer backbones. Both C_mB-PPIs and C_mB-BPIs have fully rod-like backbone structures, and thus contribution of the backbone inclination toward pretilt angles of LC molecules must be similar in both the polyimides. However, van der Waals interactions must be greater between molecular species with similar chemical structure, and the small difference might arise from closer structural similarity of the side chains of C_mB-BPIs to 5CB. The rigid parts of 5CB and side chains of C_mB-BPIs have exactly the same biphenyl group while the rigid part of C_mB-PPIs is one *p*-phenylene unit shorter than biphenyl group.

Regardless of the side chain length it was shown that in Fig. 8 that our polyimides all delivered the pretilt angles much higher than 5°, which is observed in the polyimides used in current industries [5,6]. In addition, our aromatic polyimides are highly advantageous in that the pretilt angles can be controlled by controlling their side chain structure and length by synthesis.

4. Conclusions

Two new series of polypyromellitimides having side branches consisting of both flexible *n*-alkyloxy groups and biphenylic LC moiety for application as LC-aligning layers were successfully synthesized in film form by two-step polycondensation of 3,6-bis[4′-(*n*-alkyloxy)biphenyl-4-oxy]pyromellitic dianhydrides with 1,4-phenylenediamine and biphenyl-4,4′-diamine. The new pyromellitic dianhydrides were prepared from *N*,*N*′-diphenyl-3,6-dibromopyromellitimide and sodium 4′-(*n*-alkyloxy)biphenyl-4-oxides. Inherent viscosities of the poly(amic acid)s were in the 0.26–0.62 dL/g range. Chemical structures of the polyimides were confirmed by FT-IR spectroscopy and elemental analysis. The polyimides were not soluble in common organic solvents and thermally stable. In TGA they exhibited two-step pyrolysis behaviors and in DSC they did not give any phase transitions. All polymers are not crystalline with loosely developed layer structures. LCs aligned practically vertical to the rubbing direction in the polyimides with 4′-(*n*-decyloxy)biphenyl-4-oxy and 4′-(*n*-dodecyloxy)biphenyl-4-oxy side chains and parallel to the rubbing direction in the polyimides with 4′-(*n*-hexyloxy)biphenyl-4-oxy and 4′-(*n*-octyloxy)biphenyl-4-oxy side chains. For same side chain lengths, pretilt angles of C_mB-BPIs were slightly higher than those of C_mB-PPIs.

Acknowledgements

This work was supported by the Korea Research Foundation (KRF-2004-005-D00008).

References

[1] Hergenrother PM. High Perform Polym 2003;15:3.
[2] Polyimides: fundamentals and applications. In: Ghosh MK, Mittal K, editors. New York: Marcel Dekker; 1996.
[3] Progress in polyimide chemistry I, advances in polymer science 140. In: Kricheldorf HR, editor. Progress in polyimide chemistry I, advances in polymer science 140. Berlin, Germany: Springer-Verlag; 1999.
[4] Report, Display Research, Ltd., 2003.
[5] Scheffer TJ, Nehring J. Appl Phys Lett 1984;45:1021.
[6] Handbook of liquid crystal research. In: Collings PJ, Patel JC, editors. Handbook of liquid crystal research. Oxford University Press; 1997.
[7] Lee KH, Jung JC. Polym Bull 1998;40:407.
[8] Kim DH, Jung JC. Polym Bull 2003;50:311.
[9] Lee SJ, Jung JC, Lee SW, Ree M. J Polym Sci Part A Polym Chem 2004;42:3130.
[10] Helmer-Metzmann F, Rehahn M, Schmitz L, Ballauff M, Wegner G. Makromol Chem 1992;193:1847.
[11] Jung JC, Park S-B. J Polym Sci Part A Polym Chem 1996;34:357.
[12] Park S-B, Jung JC. Makromol Chem 1992;188:2865.
[13] Lee SW, Lee SJ, Hahm SG, Lee TJ, Lee B, Chae B, et al. Macromolecules 2005;38:4331.
[14] Chae B, Kim SB, Lee SW, Kim SI, Choi W, Lee B, et al. Macromolecules 2002;35:10119.
[15] Park JH, Jung JC, Sohn BH, Lee SW, Ree M. J Polym Sci Part A Polym Chem Ed 2001;39:3622.

[16] Park JH, Jung JC, Sohn BH, Lee SW, Ree M. J Polym Sci Part A Polym Chem Ed 2001;39:1800.
[17] Lee SW, Chae B, Lee B, Choi W, Kim SB, Kim SI, et al. Chem Mater 2003;15:3105.
[18] Chae B, Lee SW, Lee B, Choi W, Kim SB, Jung YM, et al. Langmuir 2003;19:9459.
[19] Chae B, Lee SW, Lee B, Choi W, Kim SB, Jung YM, et al. J Phys Chem 2003;B-107(43):11911.
[20] Ree M, Kim K, Chang H. J Appl Phys 1997;81:698.
[21] Sugiyama T, Kuniyashi S, Seo D, Hiroyushi F, Kobayashi S. Jpn J Appl Phys 1990;29:669.
[22] Sakamoto K, Ito N, Arafune R, Ushioda S. Vib Spectrosc 1999;19: 616.
[23] Bessonov MI, Koton MM, Kudryavtsev VV, Laius LA. Polyimides thermally stable polymers. Consultants Bureau 1987;202.
[24] Park SB, Kim H, Zin WC, Jung JC. Macromolecules 1993;26:1627.